Pion-nucleus total cross sections in the (3, 3) resonance region*

A. S. Carroll, I-H. Chiang, C. B. Dover, T. F. Kycia, K. K. Li, P. O. Mazur, D. N. Michael, P. M. Mockett,† D. C. Rahm, and R. Rubinstein‡
Brookhaven National Laboratory, Upton, New York 11973
(Received 29 March 1976)

The results of total cross section measurements are presented for $\pi^{\pm}$ on targets of natural Li, C, Al, Fe, Sn, and Pb in the region of 65–320 MeV laboratory kinetic energy. The data are fitted with a simple phenomenological model, which allows one to extract the A dependence of the peak energy and width which characterize the pion-nucleus interaction.

[NUCLEAR REACTIONS $\pi^{\pm}$ on natural Li, C, Al, Fe, Sn, Pb, E =60–320 MeV; measured total σ in transmission experiment.]

There have been several recent experiments to measure pion-nucleus total cross sections on light nuclei in the energy region corresponding to the (3, 3) resonance in the elementary πN interaction.[1-4] In the present note, we present results for total cross sections σ_{tot} of $\pi^{\pm}$ *on a range of nuclei from Li to Pb*. One of the principal motivations of the experiment was to study the dependence of the position and width of the peak in σ_{tot} on target mass number A. The shift and broadening of the peak has been discussed theoretically in terms of multiple scattering effects,[5] the Pauli principle,[6] and "collisions damping" processes.[7] The latter two effects lead to modifications of the pion-nucleon amplitude in the nucleus. Calculations with simple first order optical potentials[8] [proportional to the nuclear density $\rho(r)$ times the Fermi-averaged *free space* πN amplitude] do not correctly predict the position or the width of the peak in σ_{tot}. Since the present experiment provides the first measurements involving heavy targets, the results may be useful in untangling the various competing mechanisms which shift and broaden the πN isobar in the nucleus.

We have performed measurements of the total cross sections for π^+ at 14 lab kinetic energies between 65 and 320 MeV, and for π^- at 8 energies between 80 and 320 MeV, on natural targets of Li, C, Al, Fe, Sn, and Pb. We used the same low energy separated beam from the AGS and the same detector system as in two previous experiments.[9,10] Incident pions were selected by a differential Cerenkov counter and proportional wire chamber system. The nuclear targets were 15 cm $\times$ 15 cm $\times$ 5 g/cm^2 thick, and were positioned just downstream of the liquid-hydrogen–deuterium target system used in the previous experiments. The simultaneous measurements on hydrogen and deuterium will be reported elsewhere. At each incident energy, the transmission of the beam was measured, for no target and for each of the six nuclear targets, with nine circular scintillation counters of different size. Compensation for particle absorption was made electronically.[10] The counters were always positioned corresponding to a fixed region of four-momentum transfer $|t|$ from 0.002 to 0.004 (GeV/c)^2. The total cross sections were obtained in the usual way by using a linear extrapolation to $t_i = 0$ of the partial cross sections $\sigma^{(i)}$, measured with each counter.

Before extrapolating, it was important to make corrections to the observed $\sigma^{(i)}$ to remove the effects of (1) beam decay losses $\sigma_d^{(i)}$ which were different for target and no-target measurements, and (2) Coulomb $\sigma_C^{(i)}$ and Coulomb-nuclear interference $\sigma_{CN}^{(i)}$ corrections. The values $\sigma_d^{(i)}$ were computed by a Monte Carlo method, which included the following effects: decay of pions both upstream and downstream of the targets, energy loss and multiple Coulomb scattering in the nuclear targets of both pions and muons from pion decay, and finite beam size and divergence. The effective beam size was determined for each incident energy from no-target data in both the transmission counters and a set of downstream proportional wire chambers. At a few incident energies, additional data were taken with a 0.5 g/cm^2 Sn target, a 1.2 g/cm^2 Pb target, and with the transmission counters moved to cover the region $0.003 \leq |t| \leq 0.008$ (GeV/c)^2. These data provided checks that the calculations of $\sigma_d^{(i)}$ gave the same extrapolated total cross sections for different target conditions. The relatively large distance between the Cerenkov counter and the targets (~1.6 m, because of space limitations) caused $\sigma_d^{(i)}$ to be dominated by the effect of multiple Coulomb scattering of decay muons in the targets. The corrections were typically less than 5 to 10% for Li, C, and Al, but were as large

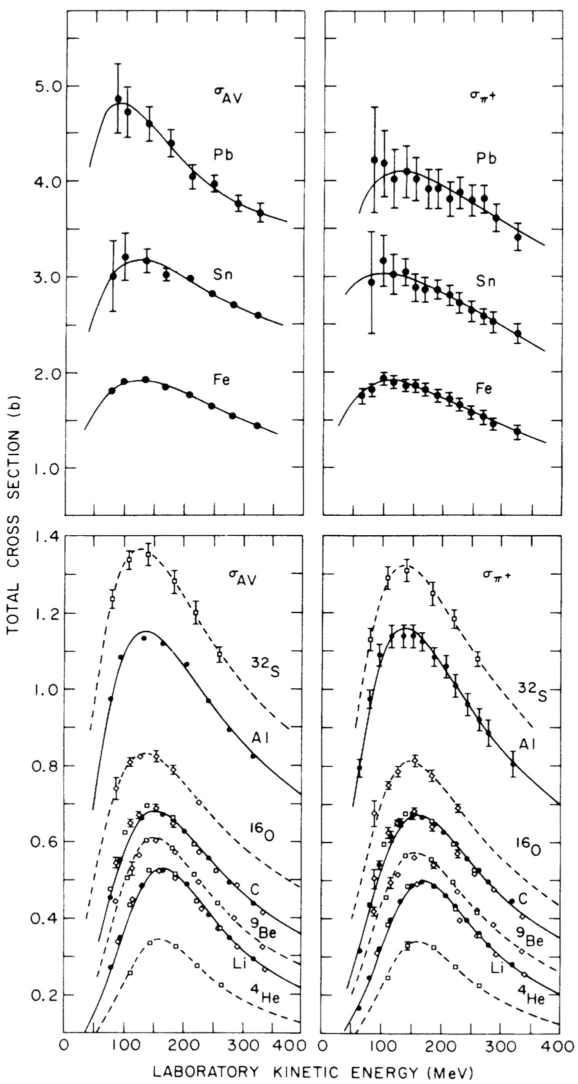

FIG. 1. Pion-nucleus total cross sections σ_{av} and σ_{π^+} in the (3,3) resonance region. The solid points are from the present experiment. The error bars include estimates of systematic uncertainties (see text). The open diamonds are from Ref. 2, the open squares are from Ref. 3. The curves are the results of fits to the data, with Eq. (2).

as 25% for Fe, 38% for Sn, and 55% for Pb.

The corrections $\sigma_C^{(i)}$ and $\sigma_{CN}^{(i)}$ were computed using an optical model prescription to generate the π-nucleus strong interaction amplitude.[11] Although the average total cross section $\sigma_{av}=(\sigma_{\pi^-}+\sigma_{\pi^+})/2$ is rather insensitive to the model used for the optical potential,[3] the cross section difference $\Delta\sigma=\sigma_{\pi^-}-\sigma_{\pi^+}$ cannot be reliably extracted from the data unless the model used to compute $\sigma_C^{(i)}$ and $\sigma_{CN}^{(i)}$ also fits the resulting extrapolated total cross sections. Using a local Laplacian potential,[8] and Fermi-averaged free space s- and p-wave π-nucleon amplitudes,[8] we found that the predicted peak positions in the nuclear total cross sections were too low in energy for the light nuclei, and the predicted widths were somewhat small. In analyzing our data, therefore, we have modified the energy and width of the effective (3,3) contribution to the optical potential to give predicted total cross sections in better agreement with the data. We have increased both the effective π-nucleon resonance energy and width, in qualitative agreement with theoretical considerations based on the effects of the Pauli principle[6] and collision damping.[7] The details of our choice of effective amplitudes and nuclear densities will be given elsewhere.[12]

The corrected nuclear total cross sections, σ_{av} and σ_{π^+}, are plotted as the solid points in Fig. 1, along with data from two previous experiments.[2,3] We are presenting average cross sections σ_{av} because their systematic uncertainty, due to Coulomb-nuclear interference, is smaller than in the individual cross sections σ_{π^+} and σ_{π^-}. Error bars are shown whenever they are larger than the plotted point; they include both statistical uncertainty and estimates of systematic uncertainties in the extrapolation procedure and in the computed corrections $\sigma_d^{(i)}$, $\sigma_C^{(i)}$, and $\sigma_{CN}^{(i)}$. Two qualitative features are evident from Fig. 1: (a) The peak position shifts downward with increasing A; (b) the peak becomes very broad for heavy nuclei.

To quantify these observations, we now develop a simple phenomenological model for pion-nucleus total cross sections. We start with the fact that the elementary resonance in the $l=1$ pion-nucleon partial wave is reflected as a peak in the cross section for *all* pion-nucleus partial waves L which contribute to the interaction[13]; that is $L \leq L_{max} \approx kR + 1$, where R is the equivalent spherical radius of the nucleus. Neglecting any smooth background contributions, we approximate σ_{tot} as a sum of contributions from each partial wave[13,14]

$$\sigma_{tot} \approx \pi \lambda\!\!\!^{-2} \sum_{L=0}^{L_{max}} \frac{(2L+1)\Gamma_1^L \Gamma^L}{[(E-E_R^L)^2+(\frac{1}{2}\Gamma^L)^2]}, \quad (1)$$

where $E=(\mu^2+k^2)^{1/2}+(M^2+k^2)^{1/2}-M+m$, M being the total nuclear mass, m the nucleon mass, and k the π-nucleus c.m. momentum ($\lambda\!\!\!^{-}=1/k$).

In Eq. (1), E_R^L is the peak energy[13] of the Lth partial wave, and Γ_1^L and Γ^L are width parameters. We parametrize E_R^L in the form[15] $E_R^L=E_0+E_1L(L+1)$. We expect an L dependence of E_R^L to arise, for instance, from the effect of the different centrifugal barriers seen by each partial wave. To restrict the number of parameters, we neglect the L dependence of the widths Γ^L and Γ_1^L. We take $\Gamma_1^L=ck$ for all L and $\Gamma^L=\Gamma_1+\Gamma_2$, where c and Γ_2

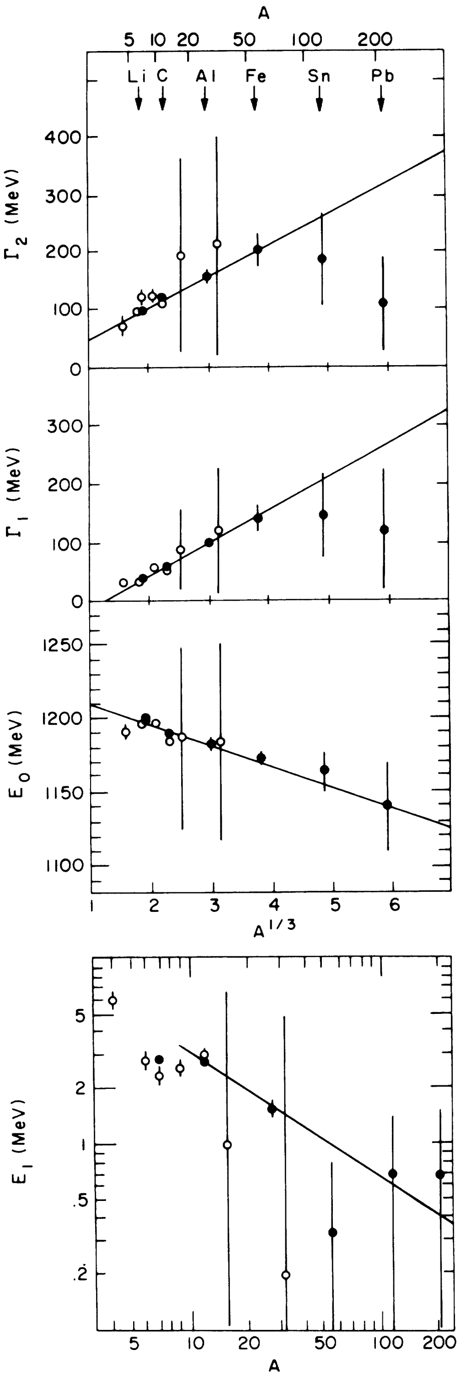

FIG. 2. The parameters E_0, E_1, Γ_1, and Γ_2 of Eq. (2), as determined by least squares fits to the average total cross section data. The solid circles are from fits to the present data; the open circles are from fits to the other data shown in Fig. 1. The solid lines represent the smooth A dependence of Eq. (4).

are constants.

For $kR \gg 1$, we can replace the sum over L in Eq. (1) by an integral. Using the above approximations for Γ_1 , Γ, and E_R^L, we find

$$\sigma_{tot}(E) \approx \frac{2\pi \lambda\!\!\!^{-2}\Gamma_1}{E_1}\left[\tan^{-1}\left(\frac{E_0+E_1L_{max}^2-E}{\frac{1}{2}\Gamma}\right) - \tan^{-1}\left(\frac{E_0-E}{\frac{1}{2}\Gamma}\right)\right]. \quad (2)$$

Expanding the right-hand side of Eq. (2) for small E_1, we arrive at the result

$$\sigma_{tot}(E) \approx \frac{\pi(R+\lambda\!\!\!^-)^2\Gamma_1\Gamma}{[(E-E_0)^2+(\frac{1}{2}\Gamma)^2]}\left(1+\frac{E_1L_{max}^2(E-E_0)}{\frac{1}{2}(\Gamma)^2}\right) \quad (3)$$

which displays the familiar Breit-Wigner form, modulated by an energy-dependent shape correction. For $E=E_0$ and $\Gamma_1 \approx \Gamma_2$, we recover the geometric limit $\sigma_{tot} \approx 2\pi(R+\lambda\!\!\!^-)^2$.

In fitting Eq. (2) to the data, we have taken the geometric size parameter R to be fixed and equal to the equivalent spherical radius of each nucleus (1.291 times the rms radius). We have used the values[16] $R=2.21$, 3.23, 3.15, 3.12, 3.19, 3.55, 3.76, 4.03, 4.97, 5.99, and 6.98 fm for ^{4}He, ^{6}Li, ^{7}Li, ^{9}Be, ^{12}C, ^{16}O, ^{27}Al, ^{32}S, ^{56}Fe, ^{120}Sn, and ^{208}Pb, respectively. The other four parameters E_0, E_1, c, and Γ_2 are allowed to vary for each nucleus, in order to obtain a best least squares fit to the data. We have fitted the other low energy data[2,3] in Fig. 1 in addition to our own. The high quality of the resultant fits using Eq. (2) are indicated by the curves in Fig. 1. The parameters E_0, E_1, Γ_1, and Γ_2 which emerge from the fits are shown in Fig. 2; Γ_1 refers to $\Gamma_1(k)$ evaluated at the momentum corresponding to E_0. The A dependence of these quantities are roughly represented by the lines shown in Fig. 2 (in MeV):

$$\begin{aligned} E_0 &\approx 1227 - 16A^{1/3}, \\ E_1 &\approx 15A^{-2/3}, \\ \Gamma_1 &\approx -67 + 54A^{1/3}, \\ \Gamma_2 &\approx -9 + 55A^{1/3}. \end{aligned} \quad (4)$$

Except for the older ^{4}He, ^{16}O, and ^{32}S data, which consists of only 5–6 points, and for Sn and Pb, which have large systematic uncertainties and do not display a clear peak, we are able to determine four parameters from our data with small error bars.

If the splitting of the peak positions in different partial waves (proportional to E_1) is due largely to the effect of the centrifugal barrier, we would expect $E_1 \sim R^{-2}$ or $E_1 \sim A^{-2/3}$. This expectation is roughly consistent with Fig. 2 [see Eq. (4)]. The fact that Γ considerably exceeds the width of the free space resonance ($\Gamma^{free} \approx 80$ MeV at peak) is due to the effects of pion absorption, quasielastic scattering, etc. If one represents all of these complicated mechanisms in a simple collision damping picture,[7] one obtains $\Gamma_2 \sim A^{1/3}$, which is approximately satisfied by the solid points in Fig. 2, at least up to $A = 56$. There is some indication of a width saturation effect for heavy nuclei. In view of the large systematic uncertainties for Sn and Pb, however, it is difficult to draw a firm conclusion.

In summary, we have measured the $\pi^{\pm}$ total cross sections on nuclear targets in the range from Li to Pb. These data enable us to reliably extract four parameters which characterize the A dependence of the pion-nucleus interaction, two of which specify the peak positions in the various contributing partial waves and another two corresponding to energy-dependent and energy-independent widths. This compact parametrization may be useful as a touchstone for establishing contact with more fundamental theories of the pion-nucleus interaction.

---

*Work supported by Energy Research and Development Administration.

†Present address: University of Washington, Seattle, Washington, 98195.

‡Present address: Fermi National Accelerator Laboratory, Batavia, Illinois, 60510.

[1]F. Binon *et al.*, Nucl. Phys. B17, 168 (1970).

[2]A. S. Clough *et al.*, Nucl. Phys. B76, 15 (1974).

[3]C. Wilkin *et al.*, Nucl. Phys. B62, 61 (1973).

[4]N. D. Gabitzsch *et al.*, Phys. Lett. 47B, 234 (1973).

[5]R. H. Landau, S. C. Phatak, and F. Tabakin, Ann. Phys. (N.Y.) 78, 299 (1973).

[6]C. B. Dover and R. H. Lemmer, Phys. Rev. C 7, 2312 (1973).

[7]D. V. Bugg, Nucl. Phys. B88, 381 (1975).

[8]For a review of such calculations, see M. M. Sternheim and R. R. Silbar, Annu. Rev. Nucl. Sci. 24, 249 (1974).

[9]A. S. Carroll *et al.*, Phys. Rev. Lett. 32, 247 (1974).

[10]A. S. Carroll *et al.*, Phys. Lett. 45B, 531 (1973).

[11]We used a modified version of the code ABACUS-M supplied by E. H. Auerbach.

[12]A. S. Carroll *et al.* (unpublished).

[13]Strictly speaking, the "bumps" which appear in each partial wave L, as per Eq. (1), are not resonances, since they do not correspond to poles of the S matrix.

[14]Note that Eq. (1) applies only to the energy region where the interaction is dominated by the (3, 3) resonance.

[15]This particular L-dependent form is suggested by a study of the partial reaction cross sections σ_R^L given by a variety of optical model calculations.

[16]R. Hofstadter and J. R. Collard, in *Landolt-Börnstein: Numerical Data and Functional Relationships in Science and Technology,* edited by K. H. Hellwege (Springer Verlag, Berlin, 1967), New Series, Group I, Vol. 2, p. 21.